

DOA ESTIMATION FOR A MULTI-FREQUENCY SIGNAL USING WIDELY-SPACED SENSORS

Tarig Ballal and C. J. Bleakley

Complex & Adaptive Systems Laboratory, School of Computer Science & Informatics, University College Dublin
Belfield, Dublin 4, Ireland

phone: + (353) 1 716 2915, fax: + (353) 1 269 7262, email: {tarig.ballal, chris.bleakley}@ucd.ie

web: <http://casl.ucd.ie/>, <http://www.csi.ucd.ie/>

ABSTRACT

The estimation of sub-sample time-delay from the phase of the cross-power spectrum (CPS) of signals received by *widely-spaced* receivers requires unwrapped phase. Conventional phase unwrapping methods require a continuous CPS that starts at zeros frequency or at a frequency with a known unwrapped phase. A novel phase unwrapping method is proposed herein that is capable of carrying out the task without these requirements. The proposed method is applied for direction-of-arrival (DOA) estimation of a bandpass signal, a case that conventional methods are unable to handle. Analytical performance and experimental results emphasize the effectiveness of the proposed method.

1. INTRODUCTION

A popular approach for DOA estimation is based on estimating the time-delay (or Time Difference Of Arrival (TDOA)) of the signal, as observed at a pair (or more) of spatially separated receivers, and then estimating the DOA by exploiting geometry (e.g., [1, 2, 3]). The most well known methods for time-delay estimation (TDE) are those based on the generalized cross correlation (GCC) [4, 5]. In general, GCC based TDE consists of weighting the Cross-Power Spectrum (CPS) of the observed signals, and transforming the resulting spectrum to the time-domain. In the time-domain, the *peak* location is taken as the time-delay estimate, which is normally an integer number of samples.

In many cases, it is more convenient to estimate the time-delay directly from the phase of the CPS in the frequency-domain. The advantage of this is in obtaining sub-sample delay estimates without resorting to intra-sample interpolation [6]. Other advantages, including optimality, are discussed in [7, 8]. In spite of this, GCC based TDE has always been more popular than direct TDE from CPS phase. The main disadvantage of estimating time-delay directly from the CPS is the requirement that phase has to be unwrapped before it can be used for TDE [7, 6]. The occurrence of phase wrapping is common when the receivers are *widely-spaced*, i.e., the receiver separation exceeds $\lambda_{min}/2$, half of the minimum wavelength of the impinging signal. In practice, wide spacing of receivers is required to enhance DOA resolution, reduce mutual coupling between receivers, or make the sensor placement physically realizable [9].

Phase Unwrapping is well known to be a difficult problem. Many phase unwrapping methods have been proposed in the literature (e.g., [2, 10, 11, 12, 13]). In general, these methods rely on the fact that the signal spectrum is continuous, and that it starts at zero frequency (i.e., the wideband signal case) or some *wrapping-free* low frequency that can be used as the starting point of the unwrapping process. The phase is unwrapped progressively starting from the lowest frequency, leaving the success of the whole process dependent on the success of the unwrapping at the low frequencies.

In some cases in practice, even the lowest frequency is subject to phase wrapping. An example of this is a bandpass signal, received by receivers whose separation exceeds $\lambda_{max}/2$, half of the *maximum* wavelength [9]. Conventional phase unwrapping methods cannot be used in this case.

In this paper, we report on a new phase unwrapping method that unwraps phase at each frequency independently (not progressively). The new method, does not require continuous phase or phase that starts from zero, and can be applied even when the phase of the lowest available frequency is uncertain. The proposed method exploits knowledge of the upper limit of the phase-frequency line slope (the maximum time-delay) to unwrap the CPS phases using a frequency pairing approach. The proposed method is capable of handling the degenerate case of the bandpass signal discussed above, which is the example considered in this paper. The proposed method can be generalized to handle the DOA spatial aliasing problem for a multi-frequency signal using non CPS based methods. Analytical performance formulae and experiments with ultrasonic signals show the effectiveness of the proposed method.

This paper is organized as follows. Section 2 describes the generic approach for DOA estimation from CPS phase. In Section 3, the proposed phase unwrapping method for two frequencies is explained. Section 4 studies the effect of noise on the proposed phase unwrapping method. In Section 5, the proposed unwrapping method is applied to DOA estimation. Experimental results are presented and discussed in Section 6, and Section 7 concludes the paper.

2. DOA ESTIMATION FROM CPS PHASE

Consider two signals received by a pair of spatially separated sensors:

$$x_1[t] = s[t] + n_1[t] \quad (1)$$

$$x_2[t] = s[t - \tau] + n_2[t] \quad (2)$$

where $s[t]$ (t represents discrete-time) is a transmitted multi-frequency signal; $n_1[t]$ and $n_2[t]$ are two random noise processes that are assumed to be uncorrelated with each other or with the transmitted signal; and τ is the delay or TDOA of $s[t]$ between the two receivers. The CPS of $x_1[t]$ and $x_2[t]$ can be estimated by dividing each of $x_1[t]$ and $x_2[t]$ into a number (N) of (possibly overlapping) frames and estimating the *complex* CPS from these frames according to [14]

$$\hat{G}_{x_1x_2}[\omega] = \frac{1}{N} \sum_{n=0}^{N-1} X_{1n}[\omega] X_{2n}^*[\omega] \quad (3)$$

where ω is the radian frequency which is assumed to be discrete; $X_{1n}[\omega]$ and $X_{2n}[\omega]$ are the discrete Fourier transforms (DFTs) of the n th frames of $x_1[t]$ and $x_2[t]$ respectively, each frame is multiplied by an appropriate window function; and “*” denotes the complex conjugate operation. The CPS $\hat{G}_{x_1x_2}[\omega]$ can be related to that of the transmitted signal by [6]

$$\hat{G}_{x_1x_2}[\omega] \approx \hat{G}_{ss}[\omega] e^{j\omega\tau + \varepsilon} \quad (4)$$

where \hat{G}_{ss} is an estimate of the *real* power spectrum of $s[t]$, and ε is a phase error due to the effect of noise, finite data record, etc.

Now, assume that there are M frequencies $\omega_m, m = 0, \dots, M-1$ in the passband. The phase at each frequency can be estimated as

$$\hat{\phi}_m = \arg(\hat{G}_{x_1 x_2}[\omega_m]) = \omega_m \tau + \varepsilon_m \quad (5)$$

where $\arg(\cdot)$ denotes the angle of a complex quantity. Considering phase wrapping, the phases in Eq. (5) can be expressed as

$$\hat{\phi}_m = [\phi_m^p + \varepsilon_m^p] + 2\pi k_m \quad (6)$$

where $k_m \in \mathbb{Z}$ are phase wrapping parameters; $[\phi_m^p + \varepsilon_m^p] \in [-\pi, \pi]$ are noisy principal phase components with ϕ_m^p being the true principal phase and ε_m^p representing the contributions of noise and estimation errors. Normally phase determination yields $[\phi_m^p + \varepsilon_m^p]$. Obtaining the true phases $\hat{\phi}_m$ (i.e., unwrapping) requires finding the correct integers k_m . It should be noted here that, in some cases, the effect of noise could result in erroneous integers k_m due to cycle slips. Herein, such effect will be ignored in order to simplify the presentation. In fact, the effect of noise in introducing cycle slips is found to be significant only at low signal-to-noise ratios (SNRs).

For a bandpass signal with the unwrapped phases given by (5), time-delay can be estimated using

$$\hat{\tau} = \frac{\sum_{m=0}^{M-1} \psi_m \hat{\phi}_m \omega_m}{\sum_{m=0}^{M-1} \psi_m \omega_m^2} \quad (7)$$

where ψ_m are generic weights (see [2, 6, 7, 8]), for which a unity value coincides with the linear least squares estimate of τ [15]. Finally, DOA is calculated from geometry as [1]

$$\hat{\theta} = \arcsin\left(\frac{c\hat{\tau}}{d}\right) \quad (8)$$

where c is the speed of propagation and d is the receivers separation.

3. PHASE UNWRAPPING FOR TWO FREQUENCY COMPONENTS

Consider two radian frequencies ω_u and ω_v . The phases of the CPS at these two frequencies following (6) are

$$\hat{\phi}_u = \phi_u^p + \varepsilon_u^p + 2\pi k_u \quad (9)$$

$$\hat{\phi}_v = \phi_v^p + \varepsilon_v^p + 2\pi k_v. \quad (10)$$

Theorem 1. *In a noise-free situation, a sufficient condition for the true phases in Eqs. (9) and (10) to be identifiable from the two principal components, is that the inter-frequency separation be less than the reciprocal of the maximum possible slope of the phase-frequency line multiplied by π , i.e. $|\omega_u - \omega_v| < \pi c/d$.*

Proof.

From the linearity of phase, we have

$$\phi_u = \phi_v \frac{\omega_u}{\omega_v}. \quad (11)$$

where ϕ_u and ϕ_v are the error-free versions of $\hat{\phi}_u$ and $\hat{\phi}_v$, respectively. By setting the noise contributions in (9) and (10) equal to zero (also ignore other sources of error), substituting Eq. (11) in (10), and subtracting the resulting equation from (9), yields

$$\phi_u = \left[\frac{\omega_u}{\omega_u - \omega_v} \right] [\phi_u^p - \phi_v^p + 2\pi k_{uv}] \quad (12)$$

where $k_{uv} \triangleq k_u - k_v$. Now phase unwrapping is transformed into a problem of determining the correct value of the integer k_{uv} . Hence, it is convenient to write (12) in the form

$$\phi_u[k] = \left[\frac{\omega_u}{\omega_u - \omega_v} \right] [\phi_u^p - \phi_v^p + 2\pi k] \quad (13)$$

where k is a general integer variable whose true value (k_{uv}) is being sought. Now, define the identifiability criterion for the true phase $\phi_u[k_{uv}]$ as being the only *valid* phase amongst the phases $\phi_u[k]$, with the validity of phase defined as falling in the interval $[-\omega_u d/c, \omega_u d/c]$. Consider the *true* phase value $\phi_u[k_{uv}]$. Any other *false* candidate value of the phase $\phi_u[k_{uv} \pm q]$, $q \in \mathbb{N}$ can be expressed, based on (13), as

$$\phi_u[k_{uv} \pm q] = \phi_u[k_{uv}] \pm 2\pi q \left[\frac{\omega_u}{\omega_u - \omega_v} \right]. \quad (14)$$

Noting that a *valid* value of the phase ϕ_u must fall in the interval $[-\omega_u d/c, \omega_u d/c]$, for $\phi_u[k_{uv} \pm q]$ to be *invalid* phases, the following inequality must be satisfied:

$$\left| \phi_u[k_{uv}] \pm 2\pi q \left[\frac{\omega_u}{\omega_u - \omega_v} \right] \right| > \omega_u \frac{d}{c}, \forall q \quad (15)$$

Considering all the sign (+/-) combinations of $\phi_u[k_{uv}]$ and $[\omega_u - \omega_v]$, a *sufficient* and *necessary* condition for the true phase to be uniquely identifiable can be stated as

$$2\pi \left| \frac{\omega_u}{\omega_u - \omega_v} \right| > \omega_u \frac{d}{c} + |\phi_u[k_{uv}]| \quad (16)$$

Since the true phase $\phi_u[k_{uv}]$ is generally unknown, it is more convenient to obtain a more strict—but accessible—version of the condition in (16) by setting $|\phi_u[k_{uv}]| = |\phi_u[k_{uv}]|_{\max} = \omega_u \frac{d}{c}$. After manipulation, this results in the *sufficient* condition

$$|\omega_u - \omega_v| < \pi \frac{c}{d} \quad (17)$$

Eq. (17) is the end of the proof of Theorem 1. In the following, we show how the condition in (17) can be exploited to identify the true value of ϕ_u . The same logic can be applied to ϕ_v , or otherwise, the true value of ϕ_v can be directly determined from the true value of ϕ_u using (11). By inspecting Eq. (13) in light of the condition in Eq. (17), we obtain

$$|\phi_u[k]| > \omega_u \frac{d}{c} \left| \frac{\phi_u^p - \phi_v^p + 2\pi k}{\pi} \right|. \quad (18)$$

It can be deduced from (18) that there are only three possible values for k that *one* of them is anticipated to yield a valid phase (i.e., $|\phi_u[k]| < \omega_u d/c$). Literally, the search has to be confined to the subset $\{-1, 0, 1\}$. The true phase can simply be identified as the minimum of a triplet.

To recover the true *noisy* phase $\hat{\phi}_u \equiv \hat{\phi}_u[k_{uv}]$ in a general case where only noisy versions of the principal phases are available (as in Eqs. (9) and (10)), and when (17) is satisfied, the following unwrapping algorithm can be used:

- I. Calculate the candidate true phases $\hat{\phi}_u[k]$ from (13) for $\{\phi_u^p, \phi_v^p\} = \{[\phi_u^p + \varepsilon_u^p], [\phi_v^p + \varepsilon_v^p]\}$ and all $k \in \{-1, 0, 1\}$.
- II. Find ϕ_u^l such that $|\phi_u^l| = \min(|\hat{\phi}_u[k]|)$, where $\min(\cdot)$ denotes the minimum value.
- III. Substitute ϕ_u^l in (9) and estimate $\hat{k}_u = \text{r}(\{\phi_u^l - [\phi_u^p + \varepsilon_u^p]\}/2\pi)$, where $\text{r}(\cdot)$ is a round-off function.
- IV. Substitute \hat{k}_u back in (9) and estimate $\hat{\phi}_u = [\phi_u^p + \varepsilon_u^p] + 2\pi \hat{k}_u$.

The objective of the last two steps is to absorb the effect of noise in the integer value representing k_{uv} . The success/failure of the above algorithm will be discussed in the following section.

4. NOISE EFFECT

In this section, the effect of noise on the performance of the proposed phase unwrapping algorithm is considered. By considering

the noise terms in Eqs. (9) and (10), one can use the same procedure used to obtain (13), to obtain the noisy version of the same equation as

$$\hat{\phi}_u[k] = \left[\frac{\omega_u}{\omega_u - \omega_v} \right] + [\phi_u^p - \phi_v^p + 2\pi k] + \varepsilon_{uv} \quad (19)$$

where $\varepsilon_{uv} = \omega_u(\varepsilon_u^p - \varepsilon_v^p)/(\omega_u - \omega_v)$ and represents the total effect of noise. For the purpose of analyzing the performance under noise, it will be assumed, without loss of generality, that ε_u^p and ε_v^p are two zero-mean Gaussian random variables with variances σ_u^2 and σ_v^2 , respectively. Hence, ε_{uv} will be a zero-mean Gaussian random variable with a variance given by

$$\sigma_{uv}^2 = \left[\frac{\omega_u}{\omega_u - \omega_v} \right]^2 [\sigma_u^2 + \sigma_v^2] \quad (20)$$

Noise can have the effect that the algorithm produces an erroneous (integer) values for k_{uv} and/or k_u , a situation which we refer to as *failure*, while producing the correct integer is referred to as *success*. First consider step II of the proposed algorithm, where a selection between three phase values is made. Each of these three phase values corresponds to an integer; the integer corresponding to the correct selection is k_{uv} ; the other two integers corresponding to the false phases will be denoted as k_1 and k_2 . The probability that step II will produce the correct answer—under noise—can therefore be written as

$$\begin{aligned} P_{s,m} &= P(|\hat{\phi}_u[k_{uv}]| < |\hat{\phi}_u[k_1]| \ \& \ |\hat{\phi}_u[k_{uv}]| < |\hat{\phi}_u[k_2]|) \\ &= P(|\phi_u[k_{uv}] + \varepsilon_{uv}| < |\phi_u[k_1] + \varepsilon_{uv}| \\ &\quad \& \ |\phi_u[k_{uv}] + \varepsilon_{uv}| < |\phi_u[k_2] + \varepsilon_{uv}|) \end{aligned} \quad (21)$$

where $\phi_u[k_{uv}]$, $\phi_u[k_1]$ and $\phi_u[k_2]$ are the noise-free candidate phases. The probability $P_{s,m}$ depends on the actual values of these phases. A procedure for evaluating $P_{s,m}$ from the cumulative distribution function (CDF) of the random variable ε_{uv} is described in Appendix A.

Now, the probability of success of step III (in restoring the correct integer k_u under noise) given the success of step II can be expressed as the probability that $\hat{k}_u = k_u$ when $\phi_u^l = \phi_u[k_{uv}] + \varepsilon_{uv}$. That can be stated as

$$P_{s,r} = P \left\{ r \left[\frac{\phi_u[k_{uv}] + \varepsilon_{uv} - (\phi_u^p + \varepsilon_u^p)}{2\pi} \right] = k_u \right\} \quad (22)$$

By substituting for $(\phi_u[k_{uv}] - \phi_u^p)/2\pi = k_u$ and manipulating, Eq.(22) reduces to

$$\begin{aligned} P_{s,r} &= P \left[-0.5 \leq \frac{\varepsilon_{uv} - \varepsilon_u^p}{2\pi} < 0.5 \right] \\ &= P[-\pi \leq \varepsilon_{uv} - \varepsilon_u^p < \pi] \\ &= \Phi_{\varepsilon_{uv} - \varepsilon_u^p}(\pi) - \Phi_{\varepsilon_{uv} - \varepsilon_u^p}(-\pi) \end{aligned} \quad (23)$$

where $\Phi_{\varepsilon_{uv} - \varepsilon_u^p}$ is the CDF of the random variable $\varepsilon_{uv} - \varepsilon_u^p$, which is has a Gaussian distribution with a zero mean and a variance equal to $\sigma_{uv}^2 + \sigma_u^2$.

Now, the probability of success for the whole algorithm presented in Section 3 will be given by

$$P_s = P_{s,m} P_{s,r} \quad (24)$$

The probability P_s is directly a function of the variances σ_u^2 and σ_v^2 . In general, for large number of frames (N), ε_u^p and ε_v^p are approximately Gaussian and $\sigma_i^2, i = u, v$ can be approximated as [6, 8]

$$\sigma_i^2 \approx \frac{1 - |\gamma[\omega_i]|^2}{2N|\gamma[\omega_i]|^2} \quad (25)$$

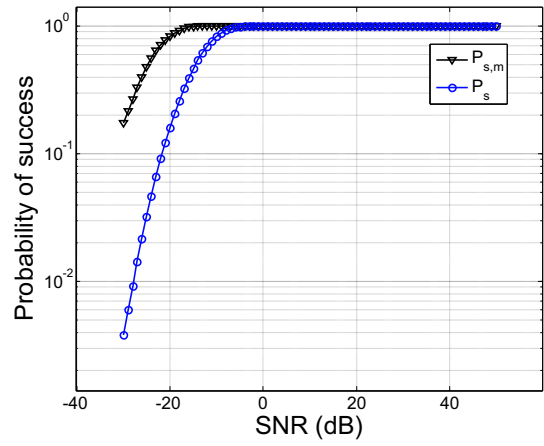


Figure 1: Probability of success of the proposed method.

where $|\gamma[\omega_i]|^2$ is the magnitude squared coherence (MSC) at frequency ω_i , which can be defined as [17]

$$|\gamma[\omega_i]|^2 = \frac{G_{ss}^2[\omega_i]}{\{G_{ss}[\omega_i] + G_{nn}[\omega_i]\}^2} \quad (26)$$

where G_{nn} is the noise power spectrum. It should be noted that Eqs. (25) and (26) rely on the assumption that the signal power is equal at the two receivers and so are the noise powers. The quantities G_{ss} and G_{nn} are generally unknown. To be able to plot P_s versus SNR, σ_u^2 and σ_v^2 must be obtained as functions of SNR. For a deterministic signal ($s[t]$), it can be shown that (see Appendix B)

$$\sigma_i^2 \approx \frac{[1 + (\alpha[\omega_i]LA)^{-1}]^2 - 1}{2N} \quad (27)$$

where $\alpha[\omega_i]$ is the ratio of the power of the received signal at the frequency ω_i to the total signal power, L is the length of the DFT and Λ is the linear SNR. It is noted that for a deterministic signal, the required parameter $\alpha[\omega_i]$ is fixed for a fixed DFT length and does not depend on the signal amplitude, hence it can be calculated directly from the DFT of a known version of the signal. This entails that the channel does not introduce any effect on the signal frequencies, which agrees with the linear channel model in (1) and (2).

By using Eq. (27) to calculate the required variances, P_s (and also $P_{s,m}$ and $P_{s,r}$) can be plotted directly against the SNR. Fig. 1 shows an example of such a plot assuming a signal $s[t]$ that is a sum of two sinusoids of frequencies, 40 and 45 kHz, and equal amplitude. The two frequencies ω_u and ω_v are selected to coincide with the two peaks of the power spectrum (which correspond to 40 and 45 kHz). The DOA of the source is assumed to be 60° . Other parameters are $d = 2\text{cm}$, $L = 32$ and $N = 20$. From Fig. 1, it can be seen that both $P_{s,m}$ and P_s fall when the SNR decreases. At low SNRs $P_{s,m}$ is better than P_s , which suggests that step II alone can be sufficient for phase unwrapping. However, the use of the whole algorithm is justified by that when outliers are discarded, the use of the whole algorithm can offer smaller error compared to step II. This can be seen from the variance of the output in the case of success of step II as given by Eq. (20), compared to that of the whole algorithm, which is expected to be equal to σ_u^2 .

5. DOA ESTIMATION WITH PHASE UNWRAPPING

To estimate the DOA of a bandpass signal utilizing the CPS, each frequency in the passband is paired with all possible frequencies such that each pair satisfies (17). For each pair, the algorithm described in Section 3 is applied on the wrapped phases obtained from

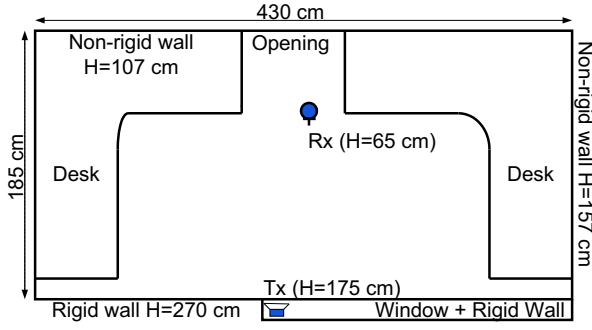


Figure 2: Test room with the locations of the transmitter (Tx) and the receivers (Rx) marked. Heights (H) are quoted between brackets.

the CPS. The pairing results in multiple estimates for the integer k_u at each frequency ω_u (see step III, Section 3). To suppress outliers, the *mode* of these estimates is taken as the final estimate of k_u . The unwrapped phase ϕ_u is calculated based on this final estimate of the integer k_u (see step IV, Section 3). Finally, the delay is estimated from the unwrapped phases using (7), and the DOA estimate is calculated from (8). In this paper, the weights ψ_m in (8) are set to a value of one.

6. EXPERIMENTAL RESULTS

The proposed approach for DOA estimation has been tested experimentally. The experiments were carried out in a normal office (see Fig. 2). Ultrasonic bandpass signals consisting of 20 equally-spaced frequencies in the range 35 - 49.5 kHz were used. The signals were constructed in a way that resembles a frequency hopping spread spectrum (FHSS) scheme [18], with a frequency duration of 3.2 ms. The sampling frequency was approximately 168 kHz. A frame size of 512 with 384 overlap between successive frames was used. A Fast Fourier Transform (FFT) was used to calculate the 512 length DFTs after windowing each frame by a Blackman window. The receivers were kept 2 cm apart (which is approximately 6 times $\lambda_{min}/2$ and 4 times $\lambda_{max}/2$), and approximately 170 cm from the transmitter. The receivers were maintained in the same location for all of the tests. Changing the angle of arrival of the signal was achieved by rotating the panel containing the two receivers. Four different angles were tested, nominally, 0° , 20° , 45° and 60° .

Fig. 3 shows examples of the unwrapped phases for each tested angle using the method described in Section 2.

Table 1 summarizes the results. The root mean square Error (RMSE) and the bias (estimated by subtracting the true angle from the mean) are used to evaluate the performance of the two proposed approaches. The results were obtained from 20 independent tests for each angle. Each test involved 3000 snapshots. The SNR was found to be approximately 30 dB. The column titled “All estimates” represents the results obtained directly from applying the proposed method. It can be seen that large error results in the cases of the *largest* tested angle— 60° . As can be seen from Fig. 3 (d), more outliers appear for this angle compared to the smaller angles. Performance can be improved by excluding the outliers from estimation of the final DOA as demonstrated in the column titled “Ex. outliers”. As it can be seen, some improvements have been obtained by applying such a two-stage approach in the larger angle cases.

To demonstrate performance at lower SNRs, artificial white Gaussian noise was added in simulation. Performance versus SNR is depicted in Fig. 4 for a DOA of 45° . The figure emphasizes the fact that outliers can dominate the performance at low SNRs, however, performance is seen to asymptotically improve as the SNR increases. The general trend in the figure is consistent with that in Fig. 1. Note that experimental results can be affected by other

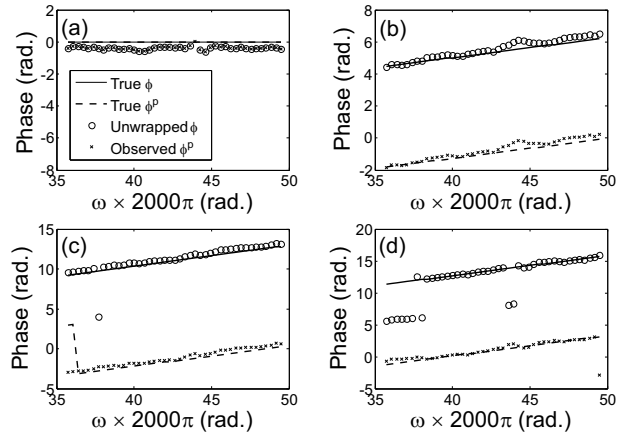


Figure 3: Experimental results: The true, true principal, observed principal and unwrapped phases for true DOA of a) 0° , b) 20° , c) 45° and d) 60° .

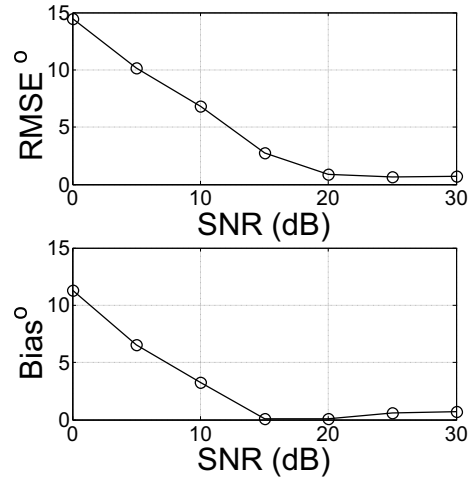


Figure 4: Performance with noise for a DOA of 45° .

factors such as reverberation.

Table 1: Experimental Results: DOA errors for 4 different angles.

DOA	All estimates		Ex. Outliers	
	Bias	RMSE	Bias	RMSE
0°	0.17°	0.76°	0.17°	0.76°
20°	-1.42°	1.42°	-1.42°	1.42°
45°	-1.33°	1.51°	-1.29°	1.30°
60°	-3.06°	4.30°	-0.00°	0.15°

7. CONCLUSION

A novel method for linear phase unwrapping, applied to DOA estimation of a multi-frequency signal received at two widely-spaced receivers, is presented. The method does not depend on the existence of unwrapped phases at low frequencies. Experimental results with ultrasonic signals emphasize the feasibility of the approach.

A. EVALUATION OF THE PROBABILITY $P_{s,m}$

First, Let us start with the probability $P(|a + \varepsilon| < |a_1 + \varepsilon|)$, where ε is a random variable with Gaussian distribution and CDF $\Phi_\varepsilon(x)$; and a and a_1 are real constants, $a \neq a_1$. This probability can be evaluated as

$$\begin{aligned} P(|a + \varepsilon| < |a_1 + \varepsilon|) &= P(\varepsilon > \zeta_1), \text{ for } a < a_1 \\ &= P(\varepsilon < \zeta_1), \text{ for } a > a_1 \end{aligned} \quad (28)$$

where $\zeta_1 \triangleq -[a + a_1]/2$. Eq. (28) is also applicable for $a_1 = a_2$, etc. Now, consider the probability $P = P(|a + \varepsilon| < |a_1 + \varepsilon| \& |a + \varepsilon| < |a_2 + \varepsilon|)$, $a \neq a_1 \neq a_2$. Based on 28, four different cases can be recognized as follows:

case 1: $a < a_1$ and $a < a_2$

$$\begin{aligned} P &= P(\varepsilon > \zeta_1 \& \varepsilon > \zeta_2) \\ &= P(\varepsilon > \max[\zeta_1, \zeta_2]) \\ &= 1 - \Phi_\varepsilon(\max[\zeta_1, \zeta_2]) \end{aligned} \quad (29)$$

case 2: $a > a_1$ and $a > a_2$

$$\begin{aligned} P &= P(\varepsilon < \zeta_1 \& \varepsilon < \zeta_2) \\ &= P(\varepsilon < \min[\zeta_1, \zeta_2]) \\ &= 1 - \Phi_\varepsilon(-\min[\zeta_1, \zeta_2]) \end{aligned} \quad (30)$$

case 3: $a < a_1$ and $a > a_2$

$$\begin{aligned} P &= P(\varepsilon > \zeta_1 \& \varepsilon < \zeta_2) \\ &= P(\varepsilon < \zeta_2) - P(\varepsilon \leq \zeta_1) \\ &= 1 - \Phi_\varepsilon(-\zeta_2) - \Phi_\varepsilon(\zeta_1), \text{ for } \zeta_1 < \zeta_2 \\ &= 0, \text{ for } \zeta_1 > \zeta_2 \end{aligned} \quad (31)$$

case 4: $a > a_1$ and $a < a_2$

$$\begin{aligned} P &= P(\varepsilon < \zeta_1 \& \varepsilon > \zeta_2) \\ &= P(\varepsilon < \zeta_1) - P(\varepsilon \leq \zeta_2) \\ &= 1 - \Phi_\varepsilon(-\zeta_1) - \Phi_\varepsilon(\zeta_2), \text{ for } \zeta_1 > \zeta_2 \\ &= 0, \text{ for } \zeta_1 < \zeta_2 \end{aligned} \quad (32)$$

where $\zeta_2 \triangleq -[a + a_2]/2$. Hence, for $P = P_{s,m}$ given by (21), the above procedure can be used by setting $a = \phi_u[k_{uv}]$, $a_1 = \phi_u[k_1]$, $a_2 = \phi_u[k_2]$ and $\varepsilon = \varepsilon_{uv}$.

B. DERIVATION OF THE VARIANCE σ_i^2 AS A FUNCTIONS OF SNR

From the definition of $|\gamma[\omega_i]|^2$ in (26)

$$\begin{aligned} \frac{1 - |\gamma[\omega_i]|^2}{|\gamma[\omega_i]|^2} &= \frac{1 - \frac{G_{ss}^2[\omega_i]}{\{G_{ss}[\omega_i] + G_{nn}[\omega_i]\}^2}}{\frac{G_{ss}^2[\omega_i]}{\{G_{ss}[\omega_i] + G_{nn}[\omega_i]\}^2}} \\ &= \frac{\{G_{ss}[\omega_i] + G_{nn}[\omega_i]\}^2 - G_{ss}^2[\omega_i]}{G_{ss}^2[\omega_i]} \\ &= \left\{ 1 + \frac{G_{nn}[\omega_i]}{G_{ss}[\omega_i]} \right\}^2 - 1 \end{aligned} \quad (33)$$

However, for white noise

$$\frac{G_{nn}[\omega_i]}{G_{ss}[\omega_i]} = \frac{\frac{P_n}{L}}{\alpha[\omega_i]P_s} = \frac{P_n}{\alpha[\omega_i]LP_s} = \{\alpha[\omega_i]L\Lambda\}^{-1} \quad (34)$$

where P_s and P_n are, respectively, the total signal power and the total noise power; $\alpha[\omega_i] \triangleq G_{ss}[\omega_i]/P_s$; L is the length of the DFT; and Λ is the linear SNR. Inserting (34) into (33), and inserting the latter back into (25), (27) is obtained.

The authors wish to thank Science Foundation Ireland (SFI) for supporting this work under grant number 06/RFP/CMS007, titled: "Robust High Precision Ultrasonic 3D Location for Ubiquitous Computing."

REFERENCES

- [1] S. Chow and P. Schultheiss, "Delay estimation using narrow-band processes," *IEEE Trans. Acoust., Speech, and Signal Process.*, vol. 27, no. 3, pp. 478–484, Jun 1981.
- [2] M. S. Brandstein J. E. Adcock, J. H. DiBiase and H. F. Silverman, "Practical issues in the use of a frequency-domain delay estimator for microphone-array applications," *Proc. the 128th Meeting of the Acoust. Soc. of Amer.*, Nov 1994.
- [3] P. Svaizer and M. Omologo, "Acoustic event localization using a crosspower-spectrum phase based technique," *Proc. the IEEE Int. Conf. on Acoust., Speech, and Signal Process.*, vol. 2, pp. 273–276, Apr 1994.
- [4] G. C. Carter, "Coherence and time delay estimation," *Proc. of the IEEE*, vol. 75, no. 2, pp. 236–255, Feb 1987.
- [5] C. Knapp and G. Carter, "The generalized correlation method for estimation of time delay," *IEEE Trans. Acoust., Speech, and Signal Process.*, vol. 24, no. 4, pp. 320–327, Aug 1976.
- [6] Y. T. Chan, R. V. Hattin and J.B. Plant, "The least squares estimation of time delay and its use in signal detection," *IEEE Trans. Acoust., Speech, and Signal Process.*, vol. 26, no. 3, pp. 217–222, Jun 1978.
- [7] B. V. Hamon and E. J. Hannan, "Spectral estimation of time delay for dispersive and non-dispersive systems," *Applied Statistics*, vol. 23, no. 2, pp. 134–142, 1973.
- [8] A. Piersol, "Time delay estimation using phase data," *IEEE Trans. Acoust., Speech, and Signal Process.*, vol. 29, no. 3, pp. 471–477, Jun 1981.
- [9] T. Ballal and C. J. Bleakley "DOA estimation of multiple sparse sources using three widely-spaced sensors," *Proc. the 17th Europ. Signal Process. Conf.*, Aug 2009.
- [10] J. M. Tribolet, "A new phase unwrapping algorithm," *IEEE Trans. Acoust., Speech, and Signal Process.*, vol. 25, no. 2, pp. 170–177, Apr 1977.
- [11] F. Bonzanigo, "An improvement of Tribolet's phase unwrapping algorithm," *IEEE Trans. Acoust., Speech, and Signal Process.*, vol. 26, no. 1, pp. 104–105, Feb 1978.
- [12] D. Li, S. Levinson "A linear phase unwrapping method for binaural sound source localization on a robot," *Proc. IEEE International Conference on Robotics and Automation*, vol. 1, pp. 19–23, Sep 2002.
- [13] I. Potamitis, H. Chen, and G. Tremoulis "Tracking of multiple moving speakers with multiple microphone arrays," *IEEE Trans. Speech and Audio Process.*, vol. 12, no. 5, pp. 520–529, Sep 2004.
- [14] J. O. Smith III, "Spectral Audio Signal Processing," *web: http://ccrma.stanford.edu/jos/sasp/*, 2009.
- [15] S. M. Kay, "Fundamentals of Statistical Signal Processing," *Printice Hall*, 1993.
- [16] A. Shapoury, "A subspace approach for DOA estimation of uniform linear arrays with increased element spacing applicable to wideband transmission," *Proc. the 2nd Int. Conf. on Broadband Networks*, vol. 2, pp. 1188–1193, Oct 2005.
- [17] G. Carter, "An overview on the time delay estimate in active and passive systems for target localization," *IEEE Trans. Acoust., Speech, and Signal Process.*, vol. 29, no. 3, pp. 527–533, Jun 1981.
- [18] R. C. Dixon, "Spread Spectrum Systems," *Jonh Wiley*, 2nd editin, 1984.